



TGA/FTIR study of the decomposition of Heet tobacco in presence of zeolites and silicate compounds

A. Marcilla^{a,b}, D. Berenguer^a

^a Inst. Univ. Ingeniería Procesos Químicos, Universidad de Alicante, 03080 Alicante, Spain

^b Dpto. Ingeniería Química, Universidad de Alicante, 03080 Alicante, Spain

ARTICLE INFO

Keywords:

TGA
FTIR
Heet tobacco
Evolved Gases
Zeolites
Silicates

ABSTRACT

This paper studied the thermal behaviour of Heet tobacco analysing the functional groups generated in the process of decomposition in inert and oxidative atmosphere. The effect of three zeolites, ZSM5, USY, and Beta, and two silicates, SBA-15 and Silica Fumed (SF) in the compounds of decomposition has been studied. The stages of decomposition of the tobacco (TGA) and the evolution of the functional groups with temperature (FTIR) have been analyzed. All additives produce significant changes in the volatiles generated under both atmospheres, being Beta zeolite and especially SBA-15 the materials more markedly reducing the yields of methylene, alcohols, CO, CO₂ and carbonyl compounds, during the pyrolysis of Heet tobacco under nitrogen and air atmospheres. This effect may contribute efficiently to further reduce the toxicity of the Heet HNB tobacco.

1. Introduction

In Heat-Not-Burn (HNB) devices the especial tobacco is not burned, but heated by a heating system that provides the required energy to form an aerosol containing nicotine together with other minor compounds [1,2]. Contrarily, smoking conventional cigarettes, where the high temperatures (up to 900 °C) reached as a consequence of tobacco combustion, leads to complex reactions and processes such as distillation pyrolysis, and combustion, producing a large number of toxic compounds in the smoke inhaled by the smokers [3]. At the low temperatures reached in HNB systems (typically below 350 °C) tobacco products are likely to undergo low temperate pyrolysis reactions. Consequently, smoke from HNB cigarettes has low content of harmful compounds (i.e.: tar and carbon monoxide) in their main stream smoke [4,5].

Reducing the toxicity of tobacco smoke or the health risk associated with tobacco smoking is a classical issue attempted by different tobacco companies and researchers. In this sense, the use of zeolites and other silica compounds for reducing the smoke toxicity has been widely studied. As an example, we would mention the studies using these types of materials attached to the filter fibers [6,7] or mixed with the tobacco cut [6,8] to reduce the presence of harmful substances in the tobacco smoke. Meier and Siegmann studied the 4% YNa zeolite/tobacco mixtures and reported decreased amounts of certain tobacco specific nitrosamines and polycyclic aromatic (PAH) compounds in tobacco smoke

[9]. Mesoporous materials by having large pore sizes (i.e.: between 5 and 20 nm) are good candidates to promote interesting cracking reactions due to the enhanced accessibility of large molecules to their active sites. For instance, Yong et al [7] used such materials for reducing the amount of PAH in tobacco smoke whereas Xu et al. [10] focused on the removal of nitrosamines from tobacco smoke. MCM-41 and SBA-15 have been the object of other interesting studies focused on reducing the tobacco smoke toxicity [11–13].

Though it is widely accepted that HNB smoking HNB tobacco represents lower health risks than conventional cigarettes, further reducing its toxicity is an issue of great interest. Nevertheless, we have found no references related to trying to attain such objective. Thus, the objective of the present study is to explore the effect of different materials, previously studied in their mixtures with conventional tobacco for reducing its toxicity, on the thermal behavior of Heet HNB tobacco under inert and oxidizing atmospheres. With this purpose, thermogravimetric analysis coupled to Fourier-transform infrared spectrometry (TGA/FTIR), as in previous works where this technique has been applied for studying tobacco, tobacco additives and catalysts [14–18], has been used.

E-mail address: antonio.marcilla@ua.es (A. Marcilla).

<https://doi.org/10.1016/j.mseb.2023.116593>

Received 8 February 2023; Received in revised form 28 March 2023; Accepted 16 May 2023

0921-5107/© 2023 The Author(s). Published by Elsevier B.V. This is an open access article under the CC BY-NC-ND license (<http://creativecommons.org/licenses/by-nc-nd/4.0/>).

2. Materials and methods

2.1. Materials

In this work we have studied the effect of three zeolites and two silicates from different sources. The zeolites ZSM5 and USY were provided by GRACE-Davison, Beta zeolite was provide by Süd-Chemie Inc. The SBA-15 mesoporous silicate, with a fibre-like morphology, was synthesised in our lab according to Zhang et al. procedure [19], and Silica Fumed (SiF) was purchased from Sigma-Aldrich. N₂ adsorption isotherms at 77 K, measured in an automatic Quantachrome AUTOSORB-6 were used to characterise the porous texture of these materials. BET Surface area was determined and the BJH model with cylindrical geometry of the pores was used to determine the pore size distributions. Total pore volumes were determined from the N₂ adsorbed at $P/P_0 = 0.965$. The acidity of these materials was determined by temperature-programmed desorption (TPD) of ammonia, using a Netzsch TG 209 thermobalance [20]. SiO₂/AlO₂ ratios were estimated by X-ray Fluorescence (XRF) [21]. Table 1 shows the characteristic of these five materials. SBA-15, as expected, shows the highest pore size, BET area and total pore volume than the zeolites. SF also shows a large pore size, though it possesses the lowest BET area. In addition, the presence of aluminium in the crystalline structure of zeolites results in a negative defect of charge that must be balanced by protons, thus generating the corresponding acidity, not present in the silicates.

Heet tobacco “amber selection” was selected for this study, and was acquired in a tobacco shop in the area. The Heet tobacco was ground and mixed with the additives with a concentration of additive of 25% w/w. A small amount of water was added to improve the mixing and obtaining a homogeneous paste. The Heet/catalyst mixtures were dried and conditioned at low temperatures (60 °C) to obtain thin sheets. The sheets obtained were crushed and sieved through a 300 µm sieve and analysed in a thermobalance coupled with a FTIR spectrophotometer. The composition of commercial Heet tobacco changes slightly according to the manufacturing batch, and with the country of sale. Table 2 shows as example the composition indicated by Philip Morris International website for consumer of tobacco amber selection manufactured for sale in Spain in August of 2021.

2.2. Tga/Ftir analysis

Samples of Heet tobacco (as a reference) and Heet tobacco-additive mixtures were placed into an alumina crucible. Sample amount ranged between 4 and 5 mg. The heating program used was as follows: 5 min at 30 °C with a flow rate of the selected gas of 80 mL min⁻¹. Following, the sample was heated from 30 to 700 °C, at heating rate of 35 °C/min with a flow of 80 mL min⁻¹ (STP). N₂ as inert atmosphere and air as oxidative atmospheres were used. The equipment employed was a Mettler Toledo TGA/DSC1 thermobalance. The TGA curves were plotted as remaining mass percentage versus temperature. And the mass time derivatives (DTG) were obtained that allow a better observation of the different

Table 1
Characteristics of the additives studied.

Material	Pore Size ^a (nm)	S _{BET} ^b (m ² /g)	V _t ^c (cm ³ /g)	SiO ₂ /Al ₂ O ₃ ratio (%w) ^d	Weak Acidity (mmol/g) ^e	Strong Acidity (mmol/g) ^e	Total Acidity (mmol/g) ^e
ZSM-5	0.51x0.55	341	0.18	22	1.2	0.8	2.0
USY	0.74	614	0.35	4.8	2.1	0	2.1
Beta	0.66x0.67 0.56x0.56	510	0.17	25	1.1	1	2.1
SBA-15	6.2	680	0.79	100% Si	0	0	0
SF	6.78	217	0.44	100% Si	0	0	0

^aPore diameter BJH method applied to the desorption branch.

^bBET surface area.

^cTotal pore volume at $P/P_0 = 0.995$.

^dXRF.

^eTPD of NH₃.

Table 2

Composition of Heet Amber selection tobacco sold in Spain.

Tobacco and ingredients ^a	mg/stick	(%)
Tobacco	177.2	66.51
Glycerol	41.1	15.43
Water	31.4	11.79
Cellulose	9.1	3.42
Guar gum	5.3	1.99
Propylene glycol	2.2	0.83
Natural & artificial flavourings	0.116	0.04

^aPhilip Morris International, <https://www.pmi.com/investor-relations/overview/making-heated-tobacco-products>.

stages of the decomposition processes occurring. The gases out of the thermobalance were transferred to a Bruker Tensor 27 FTIR spectrometer through a heated transfer line. The transfer line and the FTIR gas cell were heated at 200 °C in order to avoid the condensation of the less volatile products.

3. Results

3.1. Tga analysis

Fig. 1 shows the weight loss curves (TGA curves) and the corresponding time derivative curves (DTG curves) vs temperature, obtained from the pyrolysis of Heet tobacco and Heet tobacco/additive mixtures. All mixtures were prepared with 25% w/w additive. This amount of additive, though larger than usual additive amounts in tobacco mixtures, was used to allow a better observation of the effects of the additive on the Heet tobacco pyrolysis under both atmospheres.

The TGA and DTG curves for the thermal pyrolysis of conventional tobacco are quite complex and have been widely described previously [22–24]. At least six reaction steps, can be observed and associated to the following processes, respectively:

- Moisture evolution at temperatures lower of 100 °C.
- Glycerol and other volatile compounds evolution in the range 120–240 °C.
- Two overlapped processes corresponding to decomposition of hemicellulose and cellulose respectively, in the temperature range of 210–375 °C.
- A wide process of lignin pyrolysis at around 450 °C.
- Char dehydrogenation and aromatization reactions together with the decomposition of endogenous inorganic compounds at around 650 °C.

TGA curves corresponding to Heet tobacco and Heet tobacco/additive mixtures are shown in Fig. 1. They present similar reaction steps as conventional tobacco. All tobacco-additive mixtures present similar moisture levels of around 7%, greater than that of Heet tobacco that contains around 5% moisture (Fig. 1a). As can be seen, all zeolites

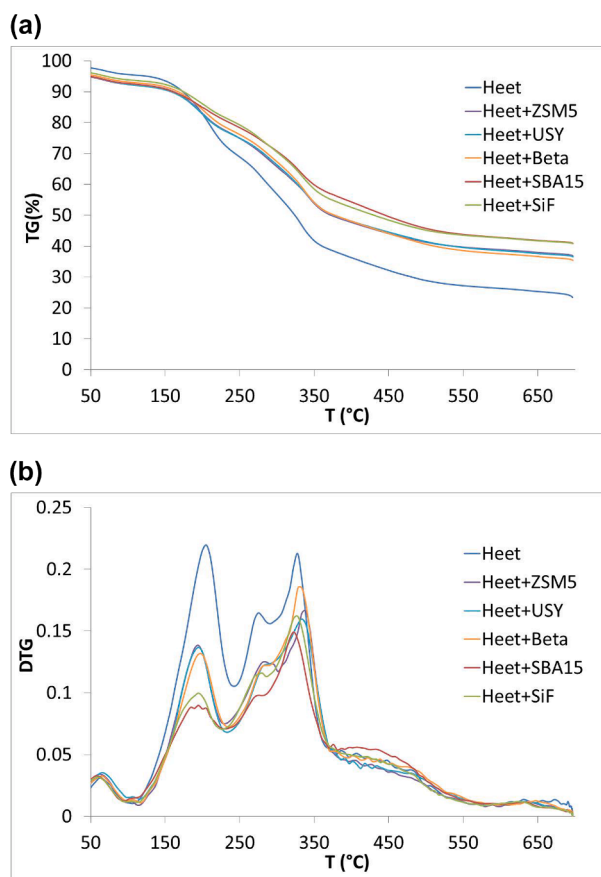


Fig. 1. TGA curves of Heet tobacco and Heet tobacco with additive; (a) under inert atmosphere, (b) under oxidative atmosphere.

present a very similar behaviour giving rise to curves that fully overlap. The same tendency can be observed for the silicates that show curves very similar but different from those shown by zeolites. Fig. 1b shows the DTG curves. The peak at 120–240 °C, associated to the evaporation of glycerol and other volatile compounds is the major peak showed by Heet tobacco, and the maximum rate of decomposition is observed at 205 °C. In the presence of the different additives, this peak decreases in similar proportion when using zeolites. As mentioned before the two silicates present a similar behavior among them, but they produce larger reductions than the zeolites, being SBA-15 the additive that shows the largest reduction. In addition, it should be mentioned that the additives produce a delay in the apparition of this peak as well as the peak is sharper, i.e.: this process seems to start a little later and end a little earlier, with the maximum rate of decomposition being observed at a temperature slightly lower than that shown by Heet tobacco. The intensity of the peak associated with the decomposition of hemicellulose (appearing at 240–290 °C) decreases in the presence of all the additives, and again SBA-15 is the material showing the larger reductions, though the peak temperatures are similar for all additives. The decomposition of the cellulose (290–375 °C) is less affected by the presence of additives than that of hemicellulose, although all additives show peak intensity reductions, and again the SBA-15 is the material that shows the greatest effect, whereas Beta zeolite is the one showing the least reduction. Finally, in the lignin decomposition occurring at around 450 °C, all additives show similar behavior reducing the weight losses.

Fig. 2 shows the TGA and DTG curves obtained under air atmosphere for Heet tobacco with and without additives. As can be seen the main difference with Fig. 1 is the presence of a new intensive peak due to the combustion of the material between 430 and 550 °C. This peak decreases notably in the presence of the additives studied, and moves towards higher temperatures, being the SBA-15, the additive decreasing

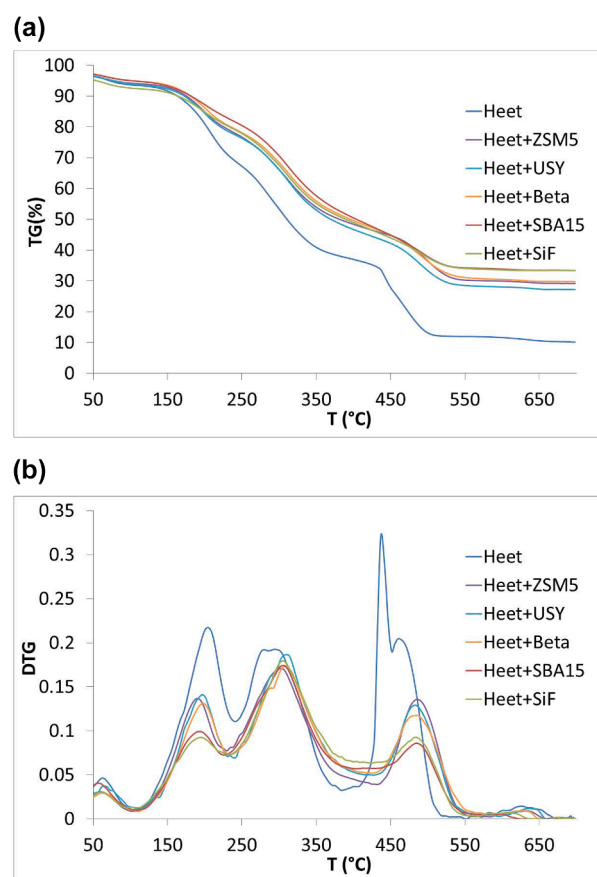


Fig. 2. TGA curves of Heet tobacco and Heet tobacco with additive; (a) under inert atmosphere, (b) under oxidative atmosphere.

that most the peak intensity. However, this range of temperature exceeds by far that normally used by HNB devices which is well below 400 °C. In the pyrolysis zone, under 400 °C, the principal differences under inert atmosphere can be observed in the double peak associated with the decomposition of hemicellulose and cellulose. Whereas in oxidative atmosphere, these two decompositions peaks overlap and practically a single decomposition peak is observed. When Heet tobacco was mixed with the different additives these peaks decreased. The major reductions are observed in presence of SF, SBA-15 and Beta zeolite. As in inert atmosphere, the peak corresponding to glycerol is clearly affected by the additives being silicates those additives that show major reductions, especially SBA-15.

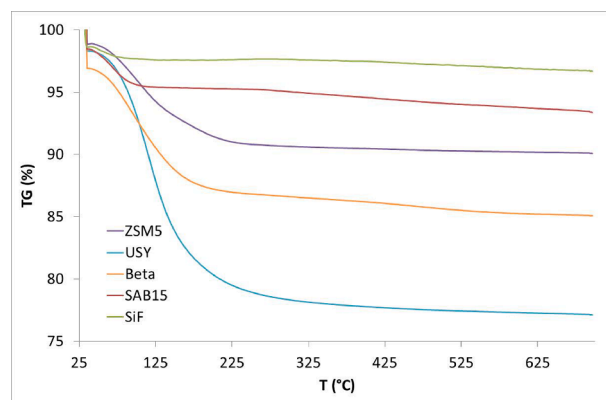


Fig. 3. TGA curves obtained for the additives under inert atmosphere.

Fig. 3 shows the weight loss of the additives when were subjected to the same temperature program. As can be seen, a weight loss around 100 °C due to the water adsorbed by these materials is observed. The amount of water adsorbed differs greatly depending on the type of material, with zeolites being the ones that show greater water content. SF is the one that has less water, 3.32 %, followed by the SBA-15 material (6.64 %). In all cases, the amount of water increases with the pore volume, though in different extent for the zeolites than for the silicates. Fig. 3 shows another process of weight loss at temperatures above 200 °C, as a consequence of the dihydroxylation of the materials. This second mass loss is generated by the condensation of silanol moieties (Si-OH) which leads to the silica densification [25]. In addition, this weight loss is lower than 2%, so the expected influence of such processes on the TG behaviour of the tobacco/additive samples should be negligible.

3.2. Ftir analysis under N₂ and air atmospheres

Fourier Transform Infrared Spectrometry (FTIR) provides qualitative information on the functional groups generated in the different stages of decomposition of the samples. A first idea of the effect of the different additives can be provided by the Gram–Schmidt curves (GS curves) that, based on vector analysis, reconstruct the acquired FTIR interferograms, allowing the plots of the FTIR signal corresponding to total evolved gases detected by the spectrometer and thus, in an indirect way, reflecting the yield of the total volatile products obtained when the temperature increases. Fig. 4 shows the normalized GS curves obtained in the absence and presence of the additives under inert and oxidative atmosphere. These normalized GS curves have been obtained by dividing each GS-intensity value by the mass of sample analysed, in this

way the results may be more representative of the products that a smoker would inhale when smoking this type of products. In general, the maxima of intensity measured in the IR cell are coincident with the maxima in the DTG curves and the overall curves are quite similar, especially under inert atmosphere (Fig. 1b and b), where the main difference is found in the peak associated with the elimination of volatile compounds (around 200 °C) that presents a significant mass loss in TGA curves with a large peak in DTG, but is not observed in the GS curves, which may be due to the glycerol condensation in the transfer line, already discussed in literature [23]. As can be seen in Fig. 4a, the material that presents the lowest formation of volatile compounds in an inert atmosphere is SBA-15, followed by Beta zeolite. In an oxidizing atmosphere (Fig. 4b), as in DTG curves two zones can be observed, the first one at temperatures below 550 °C that would be associated to the pyrolysis of tobacco and a second zone at higher temperatures marked by large and sharp peak due to the combustion of the material. As can be seen all the additives cause a delay of this second peak. Moreover, at low temperatures of decomposition, pyrolysis zone, Beta zeolite presents the lowest evolution of compounds, while the rest of the zeolites and SBA-15 present similar behaviour to that obtained from Heet tobacco. On another hand, SF seems to favor the formation of compounds in this range of temperature. But at high temperatures (combustion zone) the tendency changes and all the additives reduce the formation of volatile compounds and the SBA-15 material is the additive presenting major reductions (Fig. 4b).

Table 3 shows the assignment of the FTIR bands analysed in this work as well as the bands selected [26,27]. The evolution of the selected bands with the temperature under inert and oxidative atmosphere can be observed in Fig. 5. As can be seen in inert atmosphere, for Heet tobacco (Fig. 5a), the sum of all the bands studied gives an envelope that is similar to the Gram–Schmidt curves. In addition, it can also be observed, how the alcohol band, associated mainly with the elimination of glycerol, appears overlapped with other bands at the temperatures of decomposition of hemicellulose and cellulose, which justifies that despite being an important peak in the DTG curve, is not observed in the Gram–Schmidt curve (Fig. 4a). The most abundant band detected corresponds to CO₂, which is represented on the secondary axis for allowing

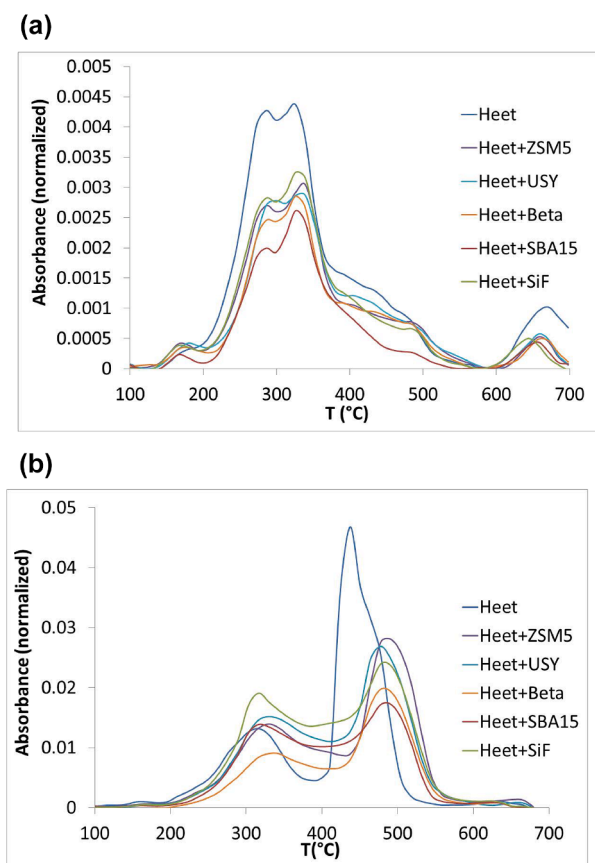


Fig. 4. Gram–Schmidt curves obtained under (a) inert atmosphere, (b) oxidative atmosphere.

Table 3
IR bands selected for the analysis of the evolution with the temperature of the decomposition gases.

Wavenumber (cm ⁻¹)	Origin	Assignment	References
2970–2950	Methyl C–H asymmetric stretch	Alkanes or alkyl substituents	[23,24]
2880–2860	Methyl C–H symmetric stretch		
1470–1430	Methyl C–H asymmetric bend		
1380–1370	Methyl C–H asymmetric bend		
2935–2915	Methyl C–H asymmetric bend		
2865–2845	Methyl C–H asymmetric bend		
1485–1445	(selected: 2968) Methylene C–H asym. stretch		
	Methylene C–H sym. stretch		
	Methylene C–H bend		
2400–2224	Asymmetrical stretching in C = O	CO ₂	[22–24]
(selected: 2361)			
2180–2108	Stretching vibration in CO	CO	[22–24]
(selected: 2195)			
1900–1600	Carbonyl groups	Aldehydes, ketones	[23,24]
(selected: 1749)			
1050–1200	C–O stretch	Alcohols, phenols	[23,24]
(selected: 1049)			

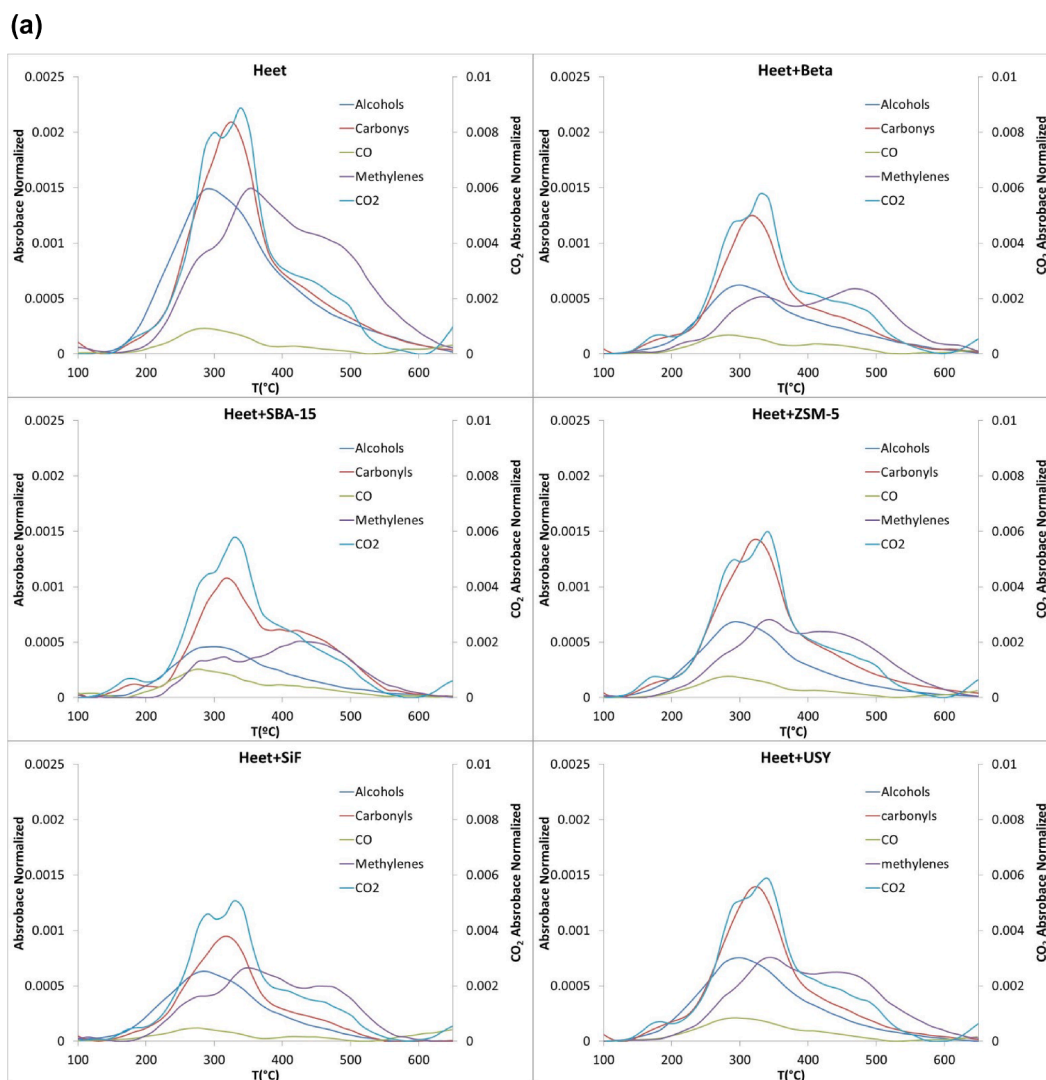


Fig. 5. Evolution of different FTIR bands with temperature for Heet tobacco with and without additives (a) under inert atmosphere, (b) under oxidative atmosphere.

better observation of the rest of the bands, followed by carbonyl bands, alcohols and methylene bands. The CO band presents much lower abundance. CO₂ band evolution shows a similar shape as that observed for the Gram–Schmidt curves, with a small peak around 200 °C due to the decomposition of volatile compounds, two important peaks between 300 and 400 °C, corresponding to the decomposition of hemicellulose and cellulose, and another peak around 450 °C due to the decomposition of lignin. Around 200 °C only CO₂ and carbonyl bands can be observed, due to the decomposition of a little part of glycerol since most of it is retained in the transfer line as arrives delayed to the FTIR cell. Moreover, all the bands studied present a major formation of compounds at the range of temperature of decomposition of hemicellulose and cellulose (300–400 °C).

As can be seen (Fig. 5a), all additives reduce the formation of alcohols, carbonyls, CO₂, and methylene, being this effect more marked for alcohols and methylene compounds. In general, silicate compounds show the larger reductions, being the zeolite Beta the one presenting the greater reductions among the zeolites. This tendency was observed in a previous work [20], where the compounds generated during the decomposition of Heet tobacco in absence and presence of these five additives were analysed in a multi-shot pyrolyzer EGA/Py-3030D at 300 °C. The results showed that this type of tobacco generates large amounts of nicotine and glycerol and compounds such as phenol,

acetaldehyde, acetone and formaldehyde and the presence of SBA-15 showed the major reductions under inert and oxidative atmospheres.

In addition, the formation of CO at temperatures lower than 400 °C (Fig. 5a) are hardly affected by the presence for zeolites, though increases slightly for the SBA-15 material and decreases for SF. Finally, it should be noted that the methylene band does not behave like the others bands, presenting broader peak with significant intensity at high temperatures. This feature can be clearly observed for Heet tobacco. The presence of the additives decrease the intensity of this peak, mainly in the zone of low temperatures, being less effective in the high temperature zone, probably corresponding to the decomposition of the lignin like material present in the sample.

Under oxidative atmosphere (Fig. 5b) the two zones obtained in GS curves can be observed, the first at temperatures below 400 °C (pyrolysis zone) and the second at high temperatures (combustion zone). As can be seen, CO₂ band has been plotted in the secondary axis to allow a better observation of the rest of the selected bands. Combustion zone is also very marked in the case of the CO band, which is slightly more abundant than aldehyde, methylene and alcohol bands for Heet tobacco, being these other bands those most abundant in the pyrolysis zone, below 400 °C. So it can be concluded that at high temperatures, practically all the tobacco was oxidised to CO₂ and CO and water. The water band has not been tracked with temperature due to the complexity of its

(b)

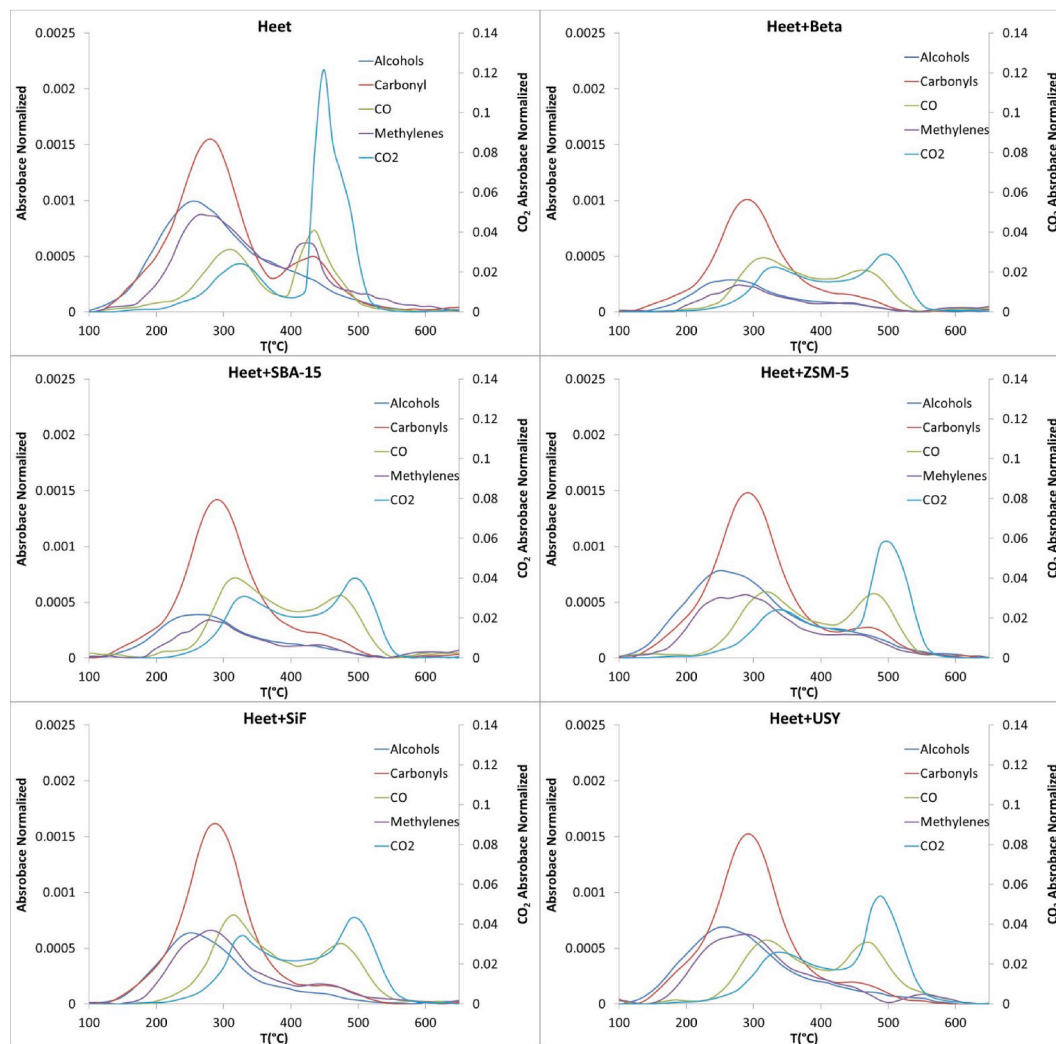
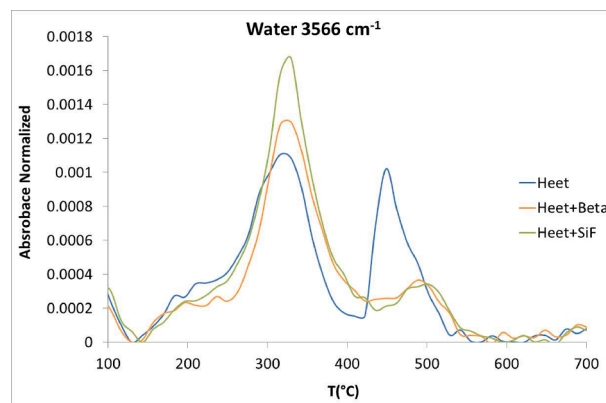


Fig. 5. (continued).

characteristic spectrum which shows a series of multiple bands centred between 1250 and 2000 cm^{-1} and 3500 – 4000 cm^{-1} . The sum of all these small bands has an important contribution to the GS curve.

Below $400\text{ }^{\circ}\text{C}$, unlike what happened under inert atmosphere, the additives only reduce the formation of alcohols and methylene, being the materials SBA-15 and specially Beta the materials that present the greatest reductions. In the carbonyl band, an important reduction is observed for the Beta material, a small reduction for SBA-15, the rest of the materials showing behaviour very similar to Heet tobacco. With respect to the formation of CO and CO_2 only Beta zeolite shows reductions, at these temperatures, while the rest of the materials show similar abundances.

It should be mentioned that Fig. 5b (FTIR bands under oxidative atmosphere) shows a significant reduction in all the bands studied when using any of the additives in the low temperature zone. However, this effect is not observed in the GS curve (Fig. 4b) where only reductions are observed for zeolite Beta. Nevertheless, this behaviour, that may lead to the erroneous conclusion that the catalyst does not reduce the emission of toxic compounds at low temperatures (Fig. 4b), is due to the important contribution of the water bands to the GS curve. Water bands are increased by the catalysts (see Fig. 6, where the band at 3566 cm^{-1} , as representative of water, is showed) leading to an increased in the GS curves, while the bands corresponding to the different functional groups are decreased.

Fig. 6. Evolution of the 3566 cm^{-1} water band under inert atmosphere.

Finally, the carbonyl, alcohol, and methylene bands, for all the samples, appear at lower temperatures under air atmosphere than under inert atmosphere, about $50\text{ }^{\circ}\text{C}$ less, while the CO and CO_2 bands appear at similar temperatures in both atmospheres. In addition, the presence of all the materials show a delay in the temperature at which tobacco combustion occurs from $435\text{ }^{\circ}\text{C}$ to $490\text{ }^{\circ}\text{C}$.

4. Conclusions

The TGA experiments show that all the additives reduce the formation of volatiles in inert and oxidative atmospheres, especially SBA15. **In both atmospheres, the presence of all materials meanly affect the peak associated with the elimination of glycerol and volatiles evolved from hemicellulose decomposition.** In addition, all additives delay the temperature at which the combustion of tobacco occurs in more than 50 °C.

FTIR analysis shows that under inert atmosphere silicates and zeolites reduce the formation of alcohols, carbonyls, CO₂, and methylene, being this effect greater for alcohols and methylene compounds, especially for SBA-15 **that reduces its formation by more than half.** Under oxidative atmosphere at low temperatures (less than 400 °C) the additives only reduce the formation of alcohols and methylene, but favour the formation of carbonyls, CO and CO₂ with the exception of Beta zeolite which reduces them slightly.

In summary, the presence of the additives studied noticeably decreased the total amount of gases generated in the decomposition of Heet tobacco under nitrogen and air atmospheres. **The evolutions with temperature of the different functional groups produced by the materials studied turn them into interesting additives for further reduce the toxicity of smoking heat not burn tobaccos such Heet tobacco, especially the SBA-15 material.**

Funding

Financial support for this investigation has been provided by the “Conselleria de Educacion, Investigacion, Cultura y Deportes” (IDI-FEDER 2018/009 and PROMETEO 2020/093).

CRedit authorship contribution statement

A. Marcilla: Conceptualization, Methodology, Supervision, Writing – review & editing, Project administration. **D. Berenguer:** Visualization, Methodology, Investigation, Validation, Data curation, Writing – original draft.

Declaration of Competing Interest

The authors declare that they have no known competing financial interests or personal relationships that could have appeared to influence the work reported in this paper.

Data availability

No data was used for the research described in the article.

References

- R. Auer, N. Conchalozano, I. Jacotsadowski, J. Cornuz, A. Berthet, Heat-not-burn tobacco cigarettes: smoke by any other name, *Jama Intern. Med.* 177 (7) (2017) 1050–1052, <https://doi.org/10.1001/jamainternmed.2017.1419>.
- E. Simonavicius, A. McNeill, L. Shahab, L.S. Brose, Heat-not-burn tobacco products: a systematic literature review, *Tob. Control* 28 (5) (2019), 582–594. <<https://doi.org/10.1136/tobaccocontrol-2018-054419>>.
- R.R. Baker, Smoke generation inside a burning cigarette: modifying combustion to develop cigarettes that may be less hazardous to health, *Prog. Energy Combust.* 32 (4) (2006) 373–385, <https://doi.org/10.1016/j.pecs.2006.01.001>.
- D.M. Burns, E. Dybing, N. Gray, S.S. Hecht, C.M. Anderson, T. Sanner, R. O'Connor, M. Djordjevic, C. Dresler, P. Hainaut, M. Jarvis, A. Opperhuizen, K. Straif, Mandated lowering of toxicants in cigarette smoke: a description of the World Health Organization TobReg proposal, *Tob. Control* 17 (2008) 132–141. <https://www.jstor.org/stable/20208394>.
- K.E. Farsalinos, N. Yannovits, T. Sarri, V. Voudris, K. Poulas, Nicotine delivery to the aerosol of a heat-not-burn tobacco product: comparison with a tobacco cigarette and e-cigarettes, *Nicotine Tob. Res.* 20 (8) (2018) 1004–1009, <https://doi.org/10.1093/ntr/ntx138>.
- J.M. Lee, J.K. Suh, S.Y. Jeong, H.K. Jin, B.K. Park, C.H. Park, J.H. Part, Manufacture of granulated complex molecular sieve composition for multiple uses, 1997, EP0857082B1.
- G. Yong, Z. Jin, H. Tong, X. Yan, G. Li, S. Liu, Selective reduction of bulky polycyclic aromatic hydrocarbons from mainstream smoke of cigarettes by mesoporous materials, *Micropor. Mesopor. Mater.* 91 (2006) 238–243, <https://doi.org/10.1016/j.micromeso.2005.12.002>.
- A. Marcilla, A. Gomez-Siurana, D. Berenguer, I. Martínez-Castellanos, M.I. Beltran, Reduction of tobacco smoke components yield in commercial cigarette brands by addition of HUSY, NaY and Al-MCM-41 to the cigarette rod, *Toxicol. Reports* 2 (2015) 152–164, <https://doi.org/10.1016/j.toxrep.2014.11.014>.
- W.M. Meier, K. Siegmann, Significant reduction of carcinogenic compounds in tobacco smoke by the use of zeolite catalysts, *Micropor. Mesopor. Mater.* 33 (1–3) (1999) 307–310, [https://doi.org/10.1016/S1387-1811\(99\)00162-6](https://doi.org/10.1016/S1387-1811(99)00162-6).
- Y. Xu, J.H. Zhu, L.L. Ma, A. Ji, Y.L. Wei, X.Y. Shang, Removing nitrosamines from mainstream smoke of cigarettes by zeolites, *Micropor. Mesopor. Mater.* 60 (2003) 125–138, [https://doi.org/10.1016/S1387-1811\(03\)00334-2](https://doi.org/10.1016/S1387-1811(03)00334-2).
- A. Marcilla, M.I. Beltran, A. Gomez-Siurana, I. Martínez, D. Berenguer, Effect of the concentration of siliceous materials added to tobacco cigarettes on the composition of the smoke generated during smoking, *Ind. Eng. Chem. Res.* 54 (2015) 1916–1929, <https://doi.org/10.1021/ie5038837>.
- A. Marcilla, M. Beltran, A. Gomez-Siurana, I. Martínez, D. Berenguer, Catalytic effect of MCM-41 on the pyrolysis and combustion processes of tobacco. Effect of the aluminum content, *Thermochim. Acta.* 518 (2011) 47–52, <https://doi.org/10.1016/j.tca.2011.02.005>.
- A. Marcilla, A. Gomez-Siurana, D. Berenguer, I. Martínez, Effect of mesoporous catalysts on the mainstream tobacco smoke of 3R4F and 1R5F reference cigarettes, *Am. J. Chem. Eng.* 3 (2015) 1–18, <https://doi.org/10.11648/j.ajche.20150301.11>.
- L. Motelica, D. Ficaí, O.C. Oprea, A. Ficaí, V.L. Ene, B.S. Vasile, E. Andronescu, A. M. Holban, Antibacterial biodegradable films based on alginate with silver nanoparticles and lemongrass essential oil-innovative packaging for cheese, *Nanomaterials* 11 (2021) 2377, <https://doi.org/10.3390/nano11092377>.
- A. Spoială, C.I. Ilie, G. Dolet, A.M. Croitoru, V.A. Surdu, R.D. Truşcă, L. Motelica, O.C. Oprea, D. Ficaí, A. Ficaí, E. Andronescu, L.M. Diţu, Preparation and characterization of chitosan/TiO₂ composite membranes as adsorbent materials for water purification, *Membranes* 12 (2022) 804, <https://doi.org/10.3390/membranes12080804>.
- J. Gao, Y. Wang, H. Hao, Investigations on dehydration processes of trisodium citrate hydrates, *Front Chem Sci Eng.* 6 (3) (2012) 276–281, <https://doi.org/10.1007/s11705-012-1206-4>.
- M. Sevilla, A.B. Fuertes, A general and facile synthesis strategy towards highly porous carbons: carbonization of organic salts, *J Mater Chem A.* 1 (2013) 13738–13741, <https://doi.org/10.1039/C3TA13149A>.
- A. Marcilla, A. Gómez, M. Beltrán, D. Berenguer, I. Martínez, I. Blasco, TGA-FTIR study of the thermal and SBA-15-catalytic pyrolysis of potassium citrate under nitrogen and air atmospheres, *J. Anal. Appl. Pyrol.* 125 (2017) 144–152, <https://doi.org/10.1016/j.jaap.2017.04.007>.
- F. Zhang, Y. Yan, H. Yang, H. Yang, Y. Meng, C. Yu, B. Tu, D. Zhao, Understanding effect of wall structure on the hydrothermal stability of mesostructured silica SBA-15, *J. Phys. Chem. B* 109 (2005) 8723–8732, <https://doi.org/10.1021/jp044632>.
- A. Marcilla, D. Berenguer, I. Martínez, Effect of the addition of zeolites and silicate compounds on the composition of the smoke generated in the decomposition of Heet tobacco under inert and oxidative atmospheres, *J. Anal. Appl. Pyrol.* 164 (2022), 105532, <https://doi.org/10.1016/j.jaap.2022.105532>.
- K. Elaiopoulos, T.h. Perraki, E. Grigoropoulou, Monitoring the effect of hydrothermal treatments on the structure of a natural zeolite through a combined XRD, FTIR, XRF, SEM and N₂-porosimetry analysis, *Micropor. Mesopor. Mater.* 134 (1–3) (2010) 29–43, <https://doi.org/10.1016/j.micromeso.2010.05.004>.
- B. Liu, Y.-M. Li, S.-B. Wu, Y.-H. Li, S.-S. Deng, Z.-L. Xia, Nanocellulose, a versatile green platform: from biosources to materials and their applications, *Bio. Resources* 8 (1) (2013) 2203–2230.
- A. Gómez-Siurana, A. Marcilla, M. Beltrán, D. Berenguer, I. Martínez-Castellanos, S. Menargues, TGA/FTIR study of tobacco and glycerol-tobacco mixtures, *Thermochim. Acta* 573 (2013) 146–157, <https://doi.org/10.1016/j.tca.2013.09.007>.
- A. Gómez-Siurana, A. Marcilla, M. Beltrán, D. Berenguer, I. Martínez-Castellanos, L. Catalá, S. Menargues, TGA/FTIR study of the MCM-41-catalytic pyrolysis of tobacco and tobacco-glycerol mixtures, *Thermochim. Acta* 587 (2014) 24–32, <https://doi.org/10.1016/j.tca.2014.04.017>.
- G. Petrişor, L. Motelica, D. Ficaí, C.I. Ilie, R.D. Truşcă, V.A. Surdu, O.C. Oprea, A. L. Miţ, G. Vasilevici, A. Semenescu, A. Ficaí, L.M. Diţu, Increasing bioavailability of trans-ferulic acid by encapsulation in functionalized mesoporous silica, *Pharmaceutics* 15 (2023) 660, <https://doi.org/10.3390/pharmaceutics15020660>.
- S. Zhou, Y. Xu, C. Wang, Z. Tian, Pyrolysis behavior of pectin under the conditions that simulate cigarette smoking, *J. Anal. Appl. Pyrolysis* 91 (2011) 232–240, <https://doi.org/10.1016/j.jaap.2011.02.015>.
- T. Ahamad, M.A. Alshehri, TG-FTIR-MS (evolved gas analysis) of bidi tobacco powder during combustion and pyrolysis, *J. Hazard. Mater.* 199–200 (2012) 200–208, <https://doi.org/10.1016/j.jhazmat.2011.10.090>.